High Zn content of Randall's plaque: A μ-X-ray fluorescence investigation

Xavier Carpentier, Dominique Bazin, Christèle Combes, Aurélie Mazouyes, Stéphan Rouzière, Pierre-Antoine Albouy, Eddy Foy, Michel Daudon

To link to this article: DOI: 10.1016/j.jtemb.2011.05.004
URL: http://dx.doi.org/10.1016/j.jtemb.2011.05.004

Pathobiochemistry

High Zn content of Randall's plaque: A μ-X-ray fluorescence investigation

Xavier Carpentier [a,b,e], Dominique Bazin [a,e,*], Christelle Combes [c,e], Aurélie Mazouyes [a,e], Stephan Rouzière [a,e], Pierre Antoine Albouy [a,e], Eddy Foy [c,e], Michel Daudon [d,e]

[a] Laboratoire de Physique des Solides, Bat 510, Université Paris XI, 91405 Orsay, France
[b] CHU Nice, Hôpital Pasteur, 30, avenue de la voie romaine, 60000 Nice, France
[c] University of Toulouse, CIRIMAT UPS-CNRS-INPT, ENSIACET, 4 allée Emile Monso, BP 44362, 31432 Toulouse Cedex 4, France
[d] Laboratoire P. Sue (CEA-CNRS) Saclay, Gif sur Yvette Cedex 91191, France
[e] Laboratoire de Biochimie A, Hôpital Necker-Enfants Malades, AP-HP, 149 Rue de Sèvres, 75743 Paris Cedex 15, France

Keywords:
Randall's plaque
Kidney stone
Oligoelements
μ-X-ray diffraction
μ-X-ray fluorescence

A B S T R A C T

Kidney stone disease, or nephrolithiasis, is a common ailment. Among the different risk factors usually associated with nephrolithiasis are dehydration, metabolic defects (especially with regard to calcium and oxalate). The presence of a mineral deposit at the surface of the renal papilla (termed Randall's plaque) has all been recently underlined. Of note, Randall's plaque is made of the calcium phosphate, carbapatite, and serves as a nucleus for kidney stone formation. The process by which apatite nanocrystals nucleate and form Randall's plaque remains unclear. This paper deals with the possible relationship between trace elements and the formation of this mineral. The investigation has been performed on a set of Randall's plaques, extracted from human kidney stones, through μ-X-ray diffraction and μ-X-ray fluorescence analyses in order to determine the chemical composition of the plaque as well as the nature and the amount of trace elements. Our data provide evidence that Zn levels are dramatically increased in carbapatite of RP by comparison to carbapatite in kidney stones, suggesting that calcified deposits within the medullar interstitium are a pathological process involving a tissue reaction. Further studies, perhaps including the investigation of biomarkers for inflammation, are necessary for clarifying the role of Zn in Randall's plaque formation.

Introduction

One of the main challenges for urology in the 21st century is to understand the biochemical mechanisms associated to the formation of Randall's plaque (RP) [1]. From an epidemiologic point of view, the proportion of kidney stones (KS) with RP markedly increased from 8.9% in the early eighties to 20.6% between 2000 and 2005 in France [2]. A parallel progression of the presence of RP at the tip of the papilla has been recently reported in the United States [3,4]. Of note, Kim et al. [5] reported that stone formation is proportional to papillary surface coverage by RP. Thus, RP can be at the origin of the significant increase of KS prevalence observed over the past two decades in industrialized countries [6–9]. More precisely, in Europe as well as in the US, 6–18% of the population, depending on the geographical region, are affected by such disease.

Since the seminal work of Randall, numerous studies have been devoted to RP [10–12]. In a recent review, we have underlined the chemical diversity of such biological samples [2]. If carbonated calcium phosphate apatite (CA) seems to be the major component of most RP, other mineral phases can be found, such as amorphous carbonated calcium phosphate (ACCP), and less frequently whitlockite or brushite. Other chemical species, namely sodium hydrogen urate and uric acid, are also observed. Such chemical diversity underlines the fact that RP have different origins [13].

Among the possible hypotheses, some trace elements may act as a catalyst. In the literature, different papers underline the fact that some elements such as Mg [14], Zn [15], Al [16,17] or Fe^{3+}-citrate complexes [18] promote or inhibit nucleation and/or crystal growth of mineral or organic species involved in urinary calculi. Also different experimental investigations [19–21] have been dedicated to the analysis of the spatial partition of trace elements inside KS by various techniques. In previous studies focused on kidney stones [22–24] we have suggested that the presence of trace elements in most cases is not a marker of an active contribution to stone formation but more probably is a consequence of a passive adsorption and/or absorption of these heavy elements respectively on and/or into crystals due to similarity of their charge and radius with calcium. Such a conclusion is in line with the fact that the medical classification [25,26] based on a relationship between the pathology and some structural characteristics of KS ignores the

* Corresponding author at: Laboratoire de Physique des Solides, Physico Chemistry institute, Bat 510, Université Paris XI, 91405 Orsay, France.
Tel.: +33 1 69 15 53 97.
E-mail address: dominique.bazin@u-psud.fr (D. Bazin).

doi:10.1016/j.jtemb.2011.05.004

Fig. 1. Typical Randall's plaque (white area) attached on a calculus made of whewellite (C1).

nature and the amount of trace elements present inside KS. To date, however, only a few experiments have directly addressed the question of whether trace elements may play a role in the formation of RP [27].

The aim of this paper is to establish whether or not there is a correlation between trace elements and RP. To do so, X-ray diffraction experiments to determine the composition of the RP as well as X-ray fluorescence measurements to identify and evaluate the amount of the trace elements have been performed. Special attention will be paid to a major oligoelement found in stones, namely Zn.

Materials and methods

Samples

RP were extracted using a stereomicroscope from seven human KS. Table 1 summarizes the chemical composition of the kidney stones as determined by Fourier Transform InfraRed (FTIR) spectroscopy. Fig. 1 shows a photo of a Randall's plaque attached to a calculus made of whewellite. All the RP were found to be composed of CA by FTIR.

The KS sample N17105, which is mainly composed of CA, which also is the primary chemical form in RP, was chosen as a reference sample in the present study.

Methods

An FTIR spectrometer Vector 22 (Bruker Spectrospin, Wissembourg, France) was used according to the analytical procedure previously described [28]. Data were collected in the absorption mode between 4000 and 400 cm^{-1} with a resolution of 4 cm^{-1}.

To obtain X-ray diffraction data on very small samples (such as RP), a special device was used. Grazing incidence small-angle X-ray scattering analysis was performed at the Laboratoire de Physique des Solides (Université Paris-Sud, France) with a home-built diffractometer using copper Kα radiation and a microfocus device. Description of the apparatus has been previously reported by Chougnet et al. [29]. Diffraction patterns were recorded on photo-sensitive image plates. After a 2D integration, classical $\theta/2\theta$-diffracted intensity representations were obtained and compared to the diffraction data collected for the CA reference kidney stone.

X-ray fluorescence experiments were performed on a RU-200B rotating anode X-ray generator at the Laboratoire Pierre Süe at the Centre d'Etudes Atomiques (LPS-CEA, Saclay, France). Runs were made at 25 mA and 45 kV molybdenum K_{α} radiation with a focal spot size of $30 \times 30\,\mu m^2$ and a dwell time of several hundreds of seconds with a germanium detector. In order to obtain an evaluation of the quantity of Zn in the samples, X-ray fluorescence spectra of a set of reference compounds made with a physical mixture of ZnO and hydroxyapatite were collected.

We use a program for X-fluorescence analysis developed at the European Synchrotron Radiation Facility (ESRF), named PyMCA [30]. First, on the NIST610 material reference and using Ca as internal reference, we found a relative error on the determination of Zn concentration about 8.7% between the Nist value and the calculated one. And then, knowing the Ca concentration deduced from C1, C2 and CA contents (Table 1), we fit the different spectra using the same program and thus we obtain the new set of data for Zn concentration in the samples.

Table 2
Zn and Sr levels in the selected biological samples.

Samples	Zn level (μg/g)	Sr level (μg/g)
CAinKS[a]	1539 ± 056	349 ± 181
RPonN4511	5056 ± 438	24 ± 2
RP on N7283	4677 ± 405	28.9 ± 0.3
RPonN10986	9948 ± 862	17 ± 2
RP on N20872	7939 ± 688	8 ± 1
RP on N26345	5559 ± 482	9 ± 1
RP on N29244	4572 ± 396	19.9 ± 0.2
RPonN42554	1903 ± 165	46 ± 1

[a] Average level of Zn and Sr measured in the reference sample (i.e. KS mainly composed of carbonated apatite).

Results and discussion

The Zn content of the different RP made of apatite and extracted from KS made of calcium oxalate is gathered in Table 2. As we can see, the Zn average level (in μg/g) measured in the different RP is $5665 \pm 490\,\mu g/g$ while the Zn level in CA stones was $1059 \pm 934\,\mu g/g$ ($p < 0.0001$) [22]. No correlation was found between the content of trace elements in RP and the chemical composition of the stone as given by FTIR. In spite of the high variability of the Zn level in the biological specimens analysed, the amount of Zn in RP appears dramatically increased by comparison with the reference CA KS.

Table 1
Morphological type and composition of the seven human kidney stones selected for the study.

Samples	Morphological type	Stone composition
Reference compound N17105	IVa	89% CA, 6% C2, 3% C1, 2% Prot
N4511	IIb, Ia, IVa	55% C1, 39% C2, 6% CA
N7283	Ia, IIb	80% C1, 12% C2, 4% CA, 2% ACCP, 2% Prot
N10986	Ia, IIb	86% C1, 11% C2, 2% CA, 1% Prot
N20872	Ia, IIb, IVa	55% C1, 40% C2, 3%CA, 2% Prot
N26345	Ia, IIb	55% C1, 42% C2, 2% CA, 1% Prot
N29244	Ia, IIb	84% C1, 11% C2, 3% CA, 2% Prot
N42554	Ia, IIb	60% C1, 35% C2, 3% CA, 2% Prot

CA, carbonated calcium hydroxylapatite; Prot, protein; C1, whewellite; C2, weddellite; ACCP, amorphous carbonated calcium phosphate.

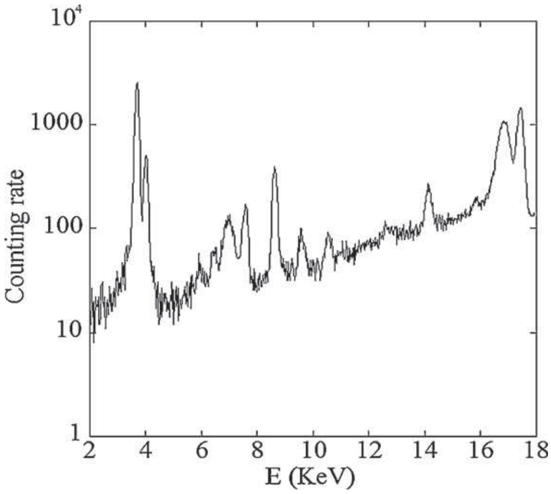

Fig. 2. Typical X-ray fluorescence spectra collected for a Randall's plaque (counting time 7200s).

From a medical point of view, pathological calcification refers to two very different entities. One is a concretion defined as a deposition of crystalline material in excretory ducts (KS but also gallstones, salivary stones, etc.) and the other one is referred to as ectopic calcification [31], defined as an inappropriate biomineralisation occurring in soft tissue (which can be related to severe pathologies like mammary or testicular cancer). Interestingly, KS belong to the first family while RP to the second one.

Fig. 2 shows that the different X-ray diffraction patterns obtained for RP are clearly similar to the one collected on a KS made of CA which is used as a reference sample in this study (sample N17105). The selected RP samples are made mostly of nanocrystalline apatite exhibiting the usual anisotropy along the *c* axis. These typical structural characteristics are associated in the X-ray diagram with a relatively fine (0 0 2) diffraction peak (at $2\theta = 26^\circ$) and several poorly resolved lines constituting a broad peak between $2\theta = 30^\circ$ and $2\theta = 35^\circ$. These structural characteristics are shared by numerous biological apatites [32,33] associated not only with pathological calcifications but also with normal ones (bone, dentine, etc.).

Of note, significant structural differences may exist among these biological apatites regarding the amount of trace elements. X-ray fluorescence [34] is a well established and powerful tool for elemental analysis of biomaterials. One important reason for this success is the fact that such experiments are non-destructive. This technique has been successfully used in several investigations of concretions such salivary [35] and gallbladder [36] stones.

In Fig. 3 are shown the X-ray fluorescence emission spectra of the different biological samples. The contribution of Ca^{2+} as well as trace elements such as Zn^{2+}, Pb^{2+} and Sr^{2+} are clearly identified by the presence of two main peaks characteristic of each of these elements. Considering our previous study dedicated to KS analysis [22] and the experimental conditions (i.e. only photons with energy higher than 3 KeV were detectable), we classified the different elements found in the kidney stone specimen as follows: first, the major element involved in the crystalline mineral phases, i.e. Ca, then trace elements such as Sr (Sr is in the same column of the periodic table as Ca), a group of transition elements including Fe, Cu, and also Zn, and finally pathological elements such as Pb. Most of the Fe present in KS probably results from residual blood at the surface or within layers of the stones (see Fig. 4).

Regarding Sr^{2+}, this element follows the same metabolic paths as Ca^{2+}. This property has been used to study calcium metabolism in idiopathic hypercalciuria by a strontium oral load test [37].

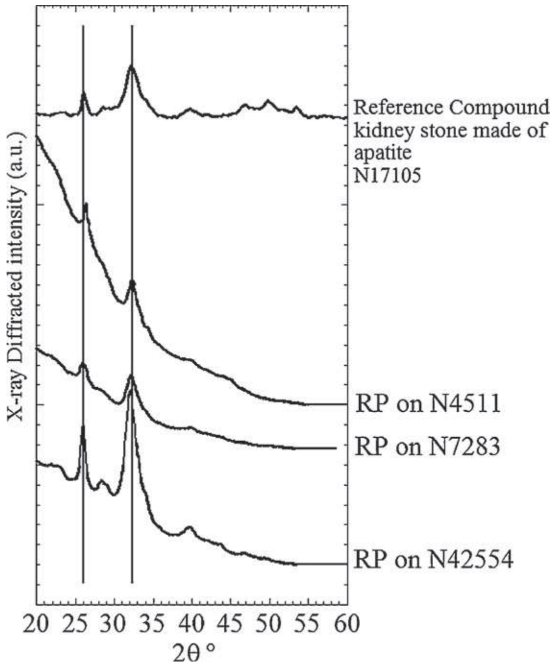

Fig. 3. X-ray diffraction diagrams collected for different RP and a KS made of apatite used as a biological apatite reference sample in this study.

Regarding their location in the body, most of the strontium cations are present in bone. Interestingly, the Sr content of RP is significantly lower than that observed in CA KS (21.8 ± 1.1 μg/g vs. 455 ± 364 μg/g, $p < 0.0001$) [22]. In the present study, we focused on the analysis of the most abundant trace element, i.e. Zn. It is well known that Zn^{2+} is an essential cofactor for the activity of more than 300 enzymes. This element is also involved in other bio-

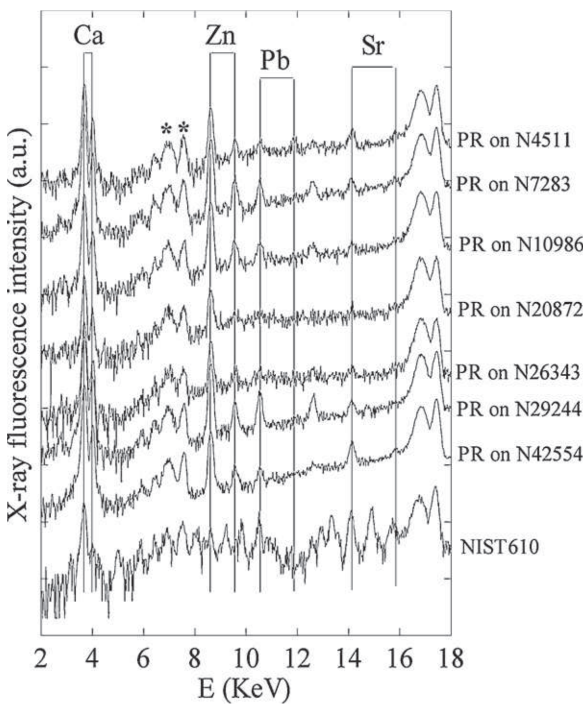

Fig. 4. Typical X-ray fluorescence spectra collected for RP and calibration compound NIST610. For RP, we can clearly see the contribution of Ca (EKα = 3691 eV, EKβ = 4012 eV), Zn (EKα = 8638 eV, EKβ = 9572 eV), Pb (ELα = 10,551 eV, ELβ = 12,613 eV) and Sr (EKα = 14,165 eV, EKβ = 15,835 eV). *Peaks corresponding to absorption by the germanium detector of the Compton and Mo Ka elastic peak.

Table 3
Amount of Zn, Sr and Pb oligoelements in kidney stones, kidney tissue and urine.

	Zn (μg/g)	Sr (μg/g)	Pb (μg/g)
CAKS[a]	1059 ± 1056	349 ± 181	62 ± 39
RP	5665 ± 490*	22 ± 13*	NA
Kidney tissue[b]	15–32	0.04–0.12	0.1–0.4
Urine[b]	0.002–0.1	0.2	0.012–0.030
Urine[c]	0.3 ± 0.2	0.14 ± 0.076	0.0013 ± 0.014

NA = not available.
[a] [22].
[b] [5] (values are ranges observed in large populations).
[c] [37].
* $p < 0.0001$ vs. CAKS.

logical functions such as nucleic acid metabolism, maintenance of membrane structure and function, hormonal activity, as well as biomineralisation. The body of adult normally contains approximately 2.2 g of Zn^{2+}. More precisely, Zn^{2+} is present in all the tissues and fluid of the body. As shown in Table 3 [38], the zinc concentration is around 15–30 μg/g in kidney tissue [39]. The biological and physical–chemical maturation of biological apatites strongly affects the uptake of trace elements. Forming crystals can easily incorporate trace elements and freshly formed apatites (immature) are less stable and more reactive than older mature mineral deposits [37]. In addition, the mineral density in freshly formed areas is also lower than that of the older ones, thus favouring ionic diffusion. Most elements will preferably react with newly formed biological apatites and if these elements remain within the apatite they will be distributed throughout the entire calcification because mineralisation will progress gradually.

However, the ability for an element to enter the apatite structure is not a good enough reason to verify its location in the mineral part of biological samples. Trace elements may also be associated with organic matrix, blood or other biological fluids, and cell constituents. Except for a very few elements like fluoride which are known to modify the mineral characteristics, it seems very difficult to determine if a particular trace element belongs to the mineral or to the organic part as most of them do not have any detectable effect on mineral structure and/or composition. Deproteinisation or demineralisation treatments of specimen are not fully reliable techniques to demonstrate the presence of trace elements in mineral or organic parts as some artefacts are possible due to the alteration of mineral or organic component reactivity, composition or structure during these treatments.

From a chemical point of view, biological apatites have been shown to easily incorporate various metals. This may be explained by their nanometer size as well as the similarity between the ion charge and size of Zn^{2+}, Sr^{2+} and Ca^{2+}. Of note, different studies [40–42] have shown that the incorporated cations (Mn^{2+}, Sr^{2+}, Pb^{2+} for example) substitute for calcium and have a tendency to occupy preferentially the Ca(II) sites in the apatite structure (vs. the Ca(I) sites).

As noticed by Li et al. [43], the substitution of the Zn^{2+} for Ca^{2+} cations causes a lower crystallinity of hydroxyapatite. Moreover, a dose-dependence effect has been pointed out by Fujii et al. [44] and Ren et al. [45]; the crystallites were smaller and of a more irregular shape as Zn level increased. In addition, chemical analysis of the cations and anions showed that Zn-containing apatites are cation deficient (Ca + Zn)/P atomic ratio < 1.67). Mayer et al. synthesised Zn-substituted carbonated hydroxyapatites and Cuisinier et al. [46] pointed out that Zn^{2+} may influence the morphology, the size and the structure (defects) of the crystals even if it is present at low levels in carbonate apatite [47,45]. Even if the mode of incorporation of Zn in apatite is not clearly understood, type II calcium sites in apatite have been shown to be the most favourable sites for Zn entering the apatite structure. Zn occurs in tetrahedral coordination and its incorporation is expected to lead to a decrease of a-lattice parameter and increase of the c-lattice parameter of the apatite [48,49].

Wu et al. [50] showed that Zn^{2+} ions are potent inhibitors of mineral formation in vitro. This result can be correlated to the in vitro study of Legeros et al. [51] regarding the precipitation of various calcium phosphates of biological interest (amorphous calcium phosphate (ACP), brushite, octacalcium phosphate (OCP), carbonated apatite) from solutions including various concentrations of Zn. They pointed out the dose-dependent effect of Zn^{2+} ions on the type and amount of calcium phosphate phases precipitated: a promotion of ACP or Zn-substituted β-tricalcium phosphate (β-TCP) formation was observed for the higher Zn^{2+} ions level tested (0.5–2 mM/L) whereas brushite, OCP and apatite formation was inhibited in the presence of a level of Zn^{2+} ions in solution as low as 0.1 mM/L. Legeros et al. [52] have also shown that Zn ions are among the ions (carbonate, magnesium and pyrophosphate ions) that most notably inhibit the crystallisation of apatite and brushite and that the combination of some of these ions can have a synergistic effect [50,51].

Zn^{2+} ions can also have an effect on the interaction between the mineral and organic phases. Fujii et al. [43] showed that due to favourable factors such as specific surface area, surface charge and pore size distribution of Zn-containing nanocrystalline apatites, the latter can selectively control the adsorption of β2-MG protein, a pathological protein in blood plasma.

To compare the Zn level in RP and in kidney stone made of carbonate apatite (Table 3), reference compounds made of a physical mixing of ZnO and synthetic industrial apatite have been prepared. Their fluorescence emission was collected in the same conditions than those used for the RP specimen analysis in order to determine the Zn amount in the selected samples. The observation of a dramatically increased Zn content in RP by comparison with the reference KS (Table 3) is highly suggestive of a relationship with an inflammatory process. Of note, numerous works have highlighted the link between zinc and inflammation [53–55].

Similarly to carbonated apatite-based kidney stones, RP exhibit higher levels of these three elements than reported in urine and kidney tissue. As observed in Table 3, the content of heavy elements is about 30–1000 times higher in RP than in urine or in kidney tissue. As a consequence, it cannot be asserted that trace elements may play a significant role in the RP formation. As previously reported [17], the spatial distribution of trace elements inside kidney stones was homogeneous. Thus the hypothesis of a passive capture of trace elements by kidney stones was finally more appropriate than a catalytic effect. At this step of discussion, our results from RP lead to a similar explanation regarding the presence of trace elements. However, we cannot confirm by our analysis that trace elements are homogeneously distributed within RP as observed in KS.

A possible way to answer this question should be based on the mapping of trace elements performed on RP obtained from kidney papilla by urological procedures. Already, we have performed an ex vivo structural investigation in order to precise the chemical nature of the RP positioned on the kidney [56].

One obvious limitation of our study is the small number of specimens investigated. Also, further studies, including histological ones and the use of biomarkers of inflammation, are needed to better clarify the role of Zn in RP formation and to understand the mechanisms involved in the genesis of RP.

Conclusion

X-ray fluorescence was used to investigate the possible role of trace elements in the genesis of RP. The nature and the content of the trace elements were obtained through X-ray fluorescence. This set of data thus opens up an interesting possibility for research in urology using X-ray-based analysis techniques related either to laboratory set up or synchrotron radiation facilities. The complete set of data shows that the levels of Zn are significantly increased in carbapatite of RP by comparison to carbapatite in kidney stones. Our results suggest that calcified deposits within the medullar interstitium, despite their high occurrence, are a pathological process.

Disclosure

All authors declared no competing of interests.

Acknowledgements

This work was supported by the physic and chemistry institutes of CNRS and by a ANR-09-BLAN-0120-02 contract.

References

[1] Randall A. An hypothesis for the origin of renal calculus. N Eng J Med 1936;111:1006–11.
[2] Daudon M, Traxer O, Jungers P, Bazin D. Stone morphology suggestive of Randall's plaque. In: Renal stone disease, AIP conference proceedings, vol. 900. 2007. p. 26–32.
[3] Low RK, Stoller ML. Endoscopic mapping of renal papillae for Randall's plaques in patients with urinary stone disease. J Urol 1997;158:2062–4.
[4] Matlaga BR, Coe FL, Evan AP, Lingeman JE. The role of Randall's plaques in the pathogenesis of calcium stones. J Urol 2007;177:31–8.
[5] Kim SC, Coe SL, Tinmouth W, et al. Stone formation is proportional to papillary surface coverage by Randall's plaque. J Urol 2005;173:117–23.
[6] Hesse A, Brandle E, Wilbert D, Kohrmann KU, Alken P. Study on the prevalence and incidence of urolithiasis in Germany comparing the years 1979 vs. 2000. Eur Urol 2003;44:709–13.
[7] Yoshida O, Terai A, Ohkawa T, Okada Y. National trend of the incidence of urolithiasis in Japan from 1965 to 1995. Kidney Int 1999;56:1899–904.
[8] Trinchieri A, Coppi F, Montanari E, Del Nero A, Zanetti G, Pisani E. Increase in the prevalence of symptomatic upper urinary tract stones during the last ten years. Eur Urol 2000;37:23–35.
[9] Stamatelou KK, Francis ME, Jones CA, Nyberg LM, Curhan GC. Time trends in reported prevalence of kidney stones in the United States: 1976–1994. Kidney Int 2003;63:1817–23.
[10] Cifuentes Delatte L, Miñon Cifuentes JL, Medina JA. New studies on papillary calculi. J Urol 1987;137:1024–9.
[11] Evan AP, Lingeman JE, Coe FL, et al. Randall's plaque of patients with nephrolithiasis begins in basement membrane of thin loops of Henle. J Clin Invest 2003;111:607–16.
[12] Evan AP, Coe FL, Lingeman JE, et al. Mechanism of formation of human calcium oxalate renal stones on Randall's plaque. Anat Rec (Hoboken) 2007;290:1315–23.
[13] Daudon M, Traxer O, Williams JC Jr, Bazin D. Randall's plaques, in: Rao Nagaraja P, Preminger GM, Kavanagh JP, editors. In Urinary Tract Stone Disease, Berlin, Springer, SBN 978-1-84800-361-3.
[14] Oka T, Yoshioka T, Koide T, Takaha M, Sonoda T. Role of magnesium in the growth of calcium oxalate monohydrate crystals. Urol Int 1987;42:89–95.
[15] Gupta A, Srivastava DK, Kumar S. Role of zinc in nephrolithiasis. J Ind Med Assoc 1984;82:235–7.
[16] Sutor DJ. Growth studies of calcium oxalate in the presence of various ions and compounds. Br J Urol 1969;41:171–85.
[17] Grases F, Genestar C, Mill A. The influence of some metallic ions and their complexes on the kinetics of crystal growth of calcium oxalate. J Cryst Growth 1989;94:507–17.
[18] Meyer JL, Thomas Jr WC. Trace metal-citric acid complexes as inhibitors of calcification and crystal growth. II. Effects of Fe(III), Cr(III) and Al(III) complexes on calcium oxalate crystal growth. J Urol 1982;128:1376–85.
[19] Pindea-Vargas CA, Eise MEM, Rodgers AL. Characterization of human kidney stones using micro-PIXE and RBS: a comparative study between two different populations. Appl Radiat Isotopes 2009;67:464–9.
[20] Chaudhri MA, Watling J, Khan FA. Spatial distribution of major elements and trace elements in bladder and kidney stone. J Radio Nucl Chem 2007;271:713–20.
[21] Rodriguez-Minon Cifuentes JL, Salvador E, Traba Villameytide ML. Usual elements in kidney stones. Actas Urol Esp 2006;30:57–62.
[22] Bazin D, Chevallier P, Matzen G, Jungers P, Daudon M. Heavy elements in urinary stones. Urol Res 2007;35:179–84.
[23] Bazin D, Carpentier X, Traxer O, Thiaudière D, Somogyi A, Reguer S, et al. Very first tests on SOLEIL regarding the Zn environment in pathological calcifications made of apatite determined by X-ray absorption spectroscopy. J Syn Rad 2008;15:506–9.
[24] Bazin D, Carpentier X, Brocheriou I, Dorfmuller P, Aubert S, Chappard Ch, et al. Biochimie 2009;91:1294–300.
[25] Daudon M, Bader CA, Jungers P. Urinary calculi: review of classification methods and correlations with etiology. Scanning Microsc 1993;7:1081–90.
[26] Daudon M, Jungers P, Bazin D. Peculiar morphology of stones in primary hyperoxaluria. N Eng J Med 2008;359:100.
[27] Bazin D, Daudon M, Chevallier P, Rouzière S, Elkaim E, Thiaudière D, et al. Les techniques de rayonnement synchrotron au service de la caractérisation d'objets biologiques: un exemple d'application, les calculs rénaux. Ann de Biol Clin 2006;64:125–39.
[28] Estepa L, Daudon M. Contribution of F.T. infrared spectroscopy to the identification of urinary stones and kidney crystal deposits. Biospectroscopy 1997;3:347–55.
[29] Chougnet A, Heitz C, Sondergard E, Berquier JM, Albouy PA, Klotz M. Substrates do influence the ordering of mesoporous thin films. J Mater Chem 2005;15:3340.
[30] Solé VA, Papillon E, Cotte M, Walter Ph, Susini J. A multiplatform code for the analysis of energy-dispersive X-ray fluorescence spectra. Spectrochim Acta Part B 2007;62:63–8.
[31] Giachelli CM. Ectopic calcification, gathering hard facts about soft tissue mineralization. Am J Pathol 1999;154:671–5.
[32] Vallet-Regı M, Gonzalez-Calbet JM. Calcium phosphates as substitution of bone tissues. Progr Sol St Chem 2004;32:1–31.
[33] Drouet C, Bosc F, Banu M, Largeot C, Combes Ch, Dechambre G, et al. Nanocrystalline apatites: from powders to biomaterials. Powder Technol 2009;190:118–22.
[34] Farquharson MJ, Al-Ebraheem A, Falkenberg G, Leek R, Harris AL, Bradley DA. The distribution of trace elements Ca, Fe, Cu and Zn and the determination of copper oxidation state in breast tumour tissue using SRXRF and XANES. Phys Med Biol 2008;53:3023–30.
[35] Zelentsov EL, Moroz TN, Kolmogorov YP, Tolmachev VE, Dragun GE, Palchik NA, et al. The elemental SRXRF analysis and mineral composition of human salivary stones. NIM A 2001;470:417–21.
[36] Ekinci N, Sahin Y. Determination of calcium and iodine in gall bladder stone using energy dispersive X-ray fluorescence spectrometry. Spectrochim Acta B 2002;57:167–71.
[37] Vezzoli G, Caumo A, Baragetti I, Zerbi S, Belinzoni P, Centemero A, et al. Study of calcium metabolism in idiopathic hypercalciuria by strontium oral load test. Clin Chem 1999;45:257–61.
[38] Komaromy-Hiller G, Owen Ash K, Costa R, Howerton K. Comparison of representative ranges based on U.S. patient population and literature reference intervals for urinary trace elements. Clin Chim Acta 2000;296: 71–90.
[39] Caroli S, Alimonti A, Coni E, Petrucci F, Senofonte O, Violante N. Occupational exposure of goldsmith workers of the area of Rome to potentially toxic metals as monitored through hair analysis. Crit Rev Anal Chem 1994;24:363–98.
[40] Bigi A, Falini G, Foresti E, Gazzano M, Ripamonti A, Roveri N. Rietveld structure refinements of calcium hydroxyapatite containing magnesium. Acta Cryst B 1996;52:87–92.
[41] Rokita E, Hermes C, Nolting HF, Ryczek J. Substitution of calcium by Sr within selected calcium phosphates. J Cryst Growth 1993;130:543–52.
[42] Sugiyama S, Moriga T, Hayashi H, Moffat JB. Characterization of Ca, Sr, Ba and Pb HAP: X-ray diffraction, photoelectron. Exafs and MAS NMR spectroscopies. Bull Chem Soc Jpn 2001;74:187–92.
[43] Li M, Xiao X, Rongfang L, Chen C, Huang L. Structural characterization of zinc-substituted hydroxyapatite prepared by hydrothermal method. J Mater Sci: Mater Med 2008;19:797–803.
[44] Fujii E, Ohkubo M, Tsuru K, Hayakawa S, Osaka A, Kawabata K, et al. Selective protein adsorption property and characterization of nano-crystalline zinc-containing hydroxyapatite. Acta Biomater 2006;2:69–74.
[45] Ren F, Xin R, Ge X, Leng Y. Characterization and structural analysis of zinc-substituted hydroxyapatites. Acta Biomater 2009;5:3141–9.
[46] Cuisinier FJG, Mayer I, Voegel JC. Microscopie électronique de haute résolution de carbonato-apatites synthétiques enrichies en zinc et en gallium. In: Mainard D, Delagoutte JP, Merle M, Louis JP, editors. In Actualités en Biomatériaux, vol. II. Paris: Romillat; 1993. p. 322–6.
[47] Mayer I, Apfelbaum F, Featherstone JD. Zinc ions in synthetic carbonated hydroxyapatites. Arch Oral Biol 1994;39:87–90.
[48] Chapell H, Shepherd D, Best S. Zinc substituted hydroxyapatite – a comparison of modelling and experimental data. Key Eng Mater 2009;396–398:729–32.
[49] Tang Y, Chapell H, Dove MT, Reeder RJ, Lee YJ. Zinc incorporation into hydroxylapatite. Biomaterials 2009;30:2864–72.
[50] Wu LNY, Genge BR, Wuthier RE. Differential effects of zinc and magnesium ions on mineralization activity of phosphatidylserine calcium phosphate complexes. J Inorg Biochem 2009;103:948–62.
[51] Legeros RZ, Bleiwas CB, Retino M, Rohanizadeh R, Legeros JP. Zinc effect on the in vitro formation of calcium phosphates: relevance to clinical inhibition of calculus formation. Am J Dent 1999;12:65–71.
[52] Legeros RZ, Mijares D, Park J, Chang XF, Khairoun I, Kijkowska R, et al. Amorphous calcium phosphates (ACP): formation and stability. Key Eng Mater 2005;284–286:7–10.
[53] Bao B, Prasad AS, Beck FW, et al. Zinc supplementation decreases oxidative stress, incidence of infection, and generation of inflammatory cytokines in sickle cell disease patients. Transl Res 2008;152:67–80.
[54] Besecker B, Bao S, Bohacova B, Papp A, Sadee W, Knoell DL. The human zinc transporter SLC39A8 (Zip8) is critical in zinc-mediated cytoprotec-

tion in lung epithelia. Am J Physiol Lung Cell Mol Physiol 2008;294: L1127–36.
[55] Haase H, Ober-Blobaum JL, Engelhardt G, et al. Zinc signals are essential for lipopolysaccharide-induced signal transduction in monocytes. J Immunol 2008;181:6491–502.
[56] Carpentier X, Bazin D, Jungers P, Reguer S, Thiaudière D, Daudon M. The pathogenesis of Randall's plaque: a papilla cartography of Ca compounds through an ex vivo investigation based on a synchrotron radiation related technique. J Synchrotron Rad 2010;17:374–9.